



CHORUS

This is the accepted manuscript made available via CHORUS. The article has been published as:

Activated scaling in disorder-rounded first-order quantum phase transitions

Arash Bellafard and Sudip Chakravarty

Phys. Rev. B **94**, 094408 — Published 7 September 2016

DOI: [10.1103/PhysRevB.94.094408](https://doi.org/10.1103/PhysRevB.94.094408)

Activated scaling in disorder rounded first-order quantum phase transitions

Arash Bellafard and Sudip Chakravarty

Department of Physics and Astronomy, University of California, Los Angeles, CA 90095, USA

(Dated: August 22, 2016)

First-order phase transitions, classical or quantum, subject to randomness coupled to energy-like variables (bond randomness) can be rounded, resulting in continuous transitions (emergent criticality). We study perhaps the simplest such model, quantum three-color Ashkin-Teller model and show that the quantum critical point in $(1+1)$ dimension is an unusual one, with activated scaling at the critical point and Griffiths-McCoy phase away from it. The behavior is similar to the transverse random field Ising model, even though the pure system has a first-order transition in this case. We believe that this fact must be attended to when discussing quantum critical points in numerous physical systems.

I. INTRODUCTION

The effect of quenched randomness on thermodynamic properties could be varied. The systems that behave less and less random at larger and larger length scales, i.e., the randomness averages out, are described by pure fixed points. On the other hand, if the randomness is competitive at all scales, the system is controlled by random fixed point and the properties of the system is altered by rare spatially localized active regions.¹⁻³ In the extreme limit, the fixed point is captured by the infinite randomness fixed point: the main features are a strong dynamical anisotropy and a broad distribution of physical quantities which is manifest through drastically different average and typical correlation functions. Some example of such systems are the quantum critical point of random quantum Ising and Potts models,⁴⁻⁷ the random singlet states of certain random antiferromagnetic spin chains,⁸⁻¹² quantum critical points separating random singlet states and the Ising antiferromagnetic phase, or the Haldane state in the random spin-1 Heisenberg chain.¹³

In addition to the singularities of the thermodynamic quantities at the quantum critical point, there is a whole parameter range around the phase transition point in which physical observables display singular and even divergent behavior in spite of a finite correlation length.^{5,14-17} Within this Griffiths-McCoy phase, there is a continuously varying dynamical exponent, z , that relates the scale of energy and length via $\varepsilon \propto \xi^{-z}$, with z diverging as $z \propto \delta^{-\psi\nu}$. Here, δ is the deviation from the critical point, ψ is some dimensionless positive constant, and ν is the correlation length exponent. A signature of the existence of infinite randomness fixed point is the divergence of the dynamical critical exponent z at the critical point, $\delta = 0$. In that case, the system exhibits *activated* dynamical scaling, $\xi_\tau \propto e^{\text{const} \times \xi^\psi}$, where ξ_τ represents a characteristic time scale of the system.

Both quantum and classical *first-order* phase transitions are ubiquitous in nature, because they do not require fine tuning of a control parameter of the system. Understanding the effect of quenched randomness that couples to energy-like variables on the thermodynamic properties of the systems that exhibit a first-order phase transition has been a challenge of experimental and theoretical studies for many years.¹⁸⁻²⁸

Here we investigate the effect of quenched disorder on the *quantum* three-color Ashkin-Teller model in $(1+1)$ dimen-

sion, which exhibits a first-order quantum phase transition in the absence of impurities. We employ discrete-time quantum Monte-Carlo method. Because there is no frustration in this system, we are able to use highly efficient cluster algorithms.²² For this disorder rounded quantum critical point, we find activated scaling at criticality and the off-critical region is characterized by Griffiths-McCoy singularities.

The outline of this paper is as follows: in the next section, we introduce the N -color quantum Ashkin-Teller model. In Sec. III, we explain how we find the critical point. We show the evidence for activated scaling in Sec. IV. Our results for correlation function and local susceptibility are presented in Sec. V and Sec. VI. Lastly, in Sec. VII we provide a discussion of our findings.

II. THE MODEL

The Hamiltonian of the N -color quantum Ashkin-Teller model in $(1+1)$ dimension is given by¹⁸

$$H = - \sum_{\alpha=1}^N \sum_{i=1}^L (J_{2,i} \sigma_{\alpha,i}^z \sigma_{\alpha,i+1}^z + h_{1,i} \sigma_{\alpha,i}^x) - \sum_{\alpha < \beta}^N \sum_{i=1}^L (J_{4,i} \sigma_{\alpha,i}^z \sigma_{\alpha,i+1}^z \sigma_{\beta,i}^z \sigma_{\beta,i+1}^z + h_{2,i} \sigma_{\alpha,i}^x \sigma_{\beta,i}^x), \quad (1)$$

where L is the length of the lattice, Greek sub-indices denote the colors, Latin sub-indices denote the lattice sites, and σ 's are the Pauli operators. The $J_{2,i}$ and $J_{4,i}$ are the random nearest-neighbor coupling constants. The $h_{1,i}$ and $h_{2,i}$ are the random transverse fields. The random coupling constants and the transverse fields are taken from a distribution restricted to only positive values. The model is self-dual, which amounts to the invariance of the Hamiltonian in Eq. (1) under the transformation $J_{2,i} \leftrightarrow h_{1,i}$, $J_{4,i} \leftrightarrow h_{2,i}$, $\mu_{\alpha,i}^x \leftrightarrow \sigma_{\alpha,i}^z \sigma_{\alpha,i+1}^z$, and $\sigma_{\alpha,i}^x \leftrightarrow \mu_{\alpha,i}^z \mu_{\alpha,i+1}^z$, where μ 's are the dual Pauli operators. The pure version of this model has been studied in the past. It is known that for $N \geq 3$, $J_{4,i}/J_{2,i} > 0$ and $h_{2,i}/h_{1,i} > 0$, there is a first-order phase transition from a paramagnetic to an ordered state.²⁹⁻³²

To study the d -dimensional quantum Hamiltonian in Eq. (1), we propose an effective classical model in $(1+1)$ dimension, where the extra imaginary time dimension is of

size $\beta \equiv 1/T$ and is divided up into $L_\tau \equiv \beta/\Delta\tau$ intervals each of width $\Delta\tau$ in the limit $\Delta\tau \rightarrow 0$. We introduce disorder only in the horizontal direction. This emulates a quenched disordered quantum system whose disorder is perfectly correlated in the imaginary time direction. Hence, we expect the behavior of this system to be in the universality class as the original quantum Ashkin-Teller model in Eq. (1). This procedure is the same as the McCoy-Wu random Ising model,^{4,10-12} which is shown to be equivalent to the random transverse field quantum spin- $\frac{1}{2}$ Ising model in the large imaginary time limit.

The partition function is $Z = \lim_{\Delta\tau \rightarrow 0} \text{Tr} e^{-S}$, with the proposed effective action given by

$$\begin{aligned} S = & - \sum_{\alpha, \tau, i} J_i S_{\alpha, i}(\tau) S_{\alpha, i+1}(\tau) \\ & - \sum_{\alpha, \tau, i} J S_{\alpha, i}(\tau) S_{\alpha, i}(\tau + 1) \\ & - \sum_{\alpha \neq \beta, i, \tau} K_i S_{\alpha, i}(\tau) S_{\beta, i}(\tau) S_{\alpha, i+1}(\tau) S_{\beta, i+1}(\tau) \\ & - \sum_{\alpha \neq \beta, i, \tau} K S_{\alpha, i}(\tau) S_{\alpha, i}(\tau + 1) S_{\beta, i}(\tau) S_{\beta, i}(\tau + 1), \end{aligned} \quad (2)$$

where the $S_i(\tau) = \pm 1$ are classical Ising spins, the indices α and β denote the colors, the index i runs over the sites of the one-dimensional lattice, and $\tau = 1, 2, \dots, L_\tau$ denotes a time slice. For computational convenience, we set $\Delta\tau = 1$ and equivalently take the limit $L_\tau \rightarrow \infty$ implying $T \rightarrow 0$. The two- and four-spin couplings, J_i and K_i , are independent of τ , because they are quenched random variables. We independently take the couplings J_i and K_i from the following rectangular distributions

$$\begin{aligned} \pi(J_i) &= \begin{cases} 1, & \text{if } J - \frac{\Delta_J}{2} < J_i < J + \frac{\Delta_J}{2} \\ 0, & \text{otherwise} \end{cases} \\ \rho(K_i) &= \begin{cases} 1, & \text{if } K - \frac{\Delta_K}{2} < K_i < K + \frac{\Delta_K}{2} \\ 0, & \text{otherwise} \end{cases} \end{aligned} \quad (3)$$

Suppose we keep one of the colors in Eq. (2) fixed, for instance $\alpha = 1$. Then, we can write the Eq. (2) as

$$\begin{aligned} S = & S_{\bar{1}} \\ & - \sum_{\tau, i} \left(J_i + \sum_{\beta \neq 1} K_i S_{\beta, i}(\tau) S_{\beta, i+1}(\tau) \right) S_{1, i}(\tau) S_{1, i+1}(\tau) \\ & - \sum_{\tau, i} \left(J + \sum_{\beta \neq 1} K S_{\beta, i}(\tau) S_{\beta, i}(\tau + 1) \right) S_{1, i}(\tau) S_{1, i}(\tau + 1), \end{aligned} \quad (4)$$

where the first term, $S_{\bar{1}}$, does not contain the color 1. The second and third terms of the Eq. (4) can be regarded as the Ising model action with coupling constants $J_i + \sum_{\beta \neq 1} K_i S_{\beta, i}(\tau) S_{\beta, i+1}(\tau)$ in the spatial direction and $J + \sum_{\beta \neq 1} K S_{\beta, i}(\tau) S_{\beta, i}(\tau + 1)$ in the temporal direction. We can implement any cluster Monte-Carlo algorithm suited for

the Ising model. We use the generalization of the Swendsen-Wang³³ cluster Monte-Carlo algorithm suggested by Niedermayer.³⁴

In our simulation on a square lattice of size $L \times L_\tau$ we use periodic boundary conditions in both spatial and imaginary time directions. The equilibration “time” is estimated using the logarithmic binning method, i.e., we compare the average values of each observable over 2^n Monte-Carlo steps and make sure that the last three averages are within each others error bars. Each observable is obtained by averaging over 10000 disordered configurations and for each disordered configuration, 10000 thermal averages is conducted. The error bars are calculated using the Jackknife procedure.³⁵⁻³⁷

III. CRITICAL POINT

We estimate the location of the quantum critical point along the analysis of Rieger and Young³⁸ for the quantum spin glass systems using the magnetic Binder cumulant³⁹

$$V_m = 1 - \frac{[(m^4)]}{3[(m^2)^2]}, \quad (5)$$

where

$$m = \frac{1}{L_\tau L} \left[\left\langle \sum_{\alpha} |m_{\alpha}| \right\rangle \right], \quad (6)$$

with $m_{\alpha} = \sum_{\tau, i} S_{\alpha, i}(\tau)$. The square and angular brackets, $[\dots]$ and $\langle \dots \rangle$, denote the disorder and thermal averages, respectively. In the disordered phase, $V_m \propto L^{-d} \rightarrow 0$ as $L \rightarrow \infty$.^{40,41} In the ordered phase, we have spontaneous magnetization at $\pm m$ and $V_m \rightarrow 2/3$ as $L \rightarrow \infty$.^{40,41} Furthermore, in the paramagnetic phase, for small L_τ , the system is disordered and effectively classical at a finite temperature, therefore $V_m \rightarrow 0$. For $L_\tau \rightarrow \infty$, the system is quasi one-dimensional in the imaginary time direction, therefore $V_m \rightarrow 0$ also. There exists an intermediate point where V_m acquires a maximum value V_m^{\max} . This maximum value decreases as L increases if the system is in the paramagnetic phase, whereas it increases as L increases if the system is in the ferromagnetic phase. There is an intermediate point at which the V_m^{\max} is a constant for all L which is the quantum critical point; see Fig. 1A. For our model with the parameter set $(K, \Delta_K, \Delta_J) = (0.08, 0.04, 0.2)$, we estimate the critical point to be $J_c = 0.245 \pm 0.001$.

We also found the critical point of the system with the parameter set $(K, \Delta_K, \Delta_J) = (0.1, 0.05, 0.2)$, with $J_c = 0.205 \pm 0.002$. Careful analyses of two parameter sets $(K, \Delta_K, \Delta_J) = (0.08, 0.04, 0.2)$ and $(0.1, 0.05, 0.2)$ yielded very similar results. Henceforth, we will be reporting only on the former parameter set in the rest of our paper.

IV. FINITE-SIZE SCALING

The Binder cumulant (5) has the finite-size scaling form³⁹

$$V_m = \mathcal{V} \left(\frac{J - J_c}{J_c} L^{1/\nu}, \frac{L_\tau}{L^z} \right). \quad (7)$$

As shown in Fig. 1A, the value of V_m^{\max} at the critical point is independent of the system size L and L_τ at the maximum varies as L^z . Therefore, we naively would expect that a plot of the V_m against L_τ/L_τ^{\max} at the critical point should collapse the data, but from Fig. 1B we see that it does not. In contrast, if we assume that the logarithm of the characteristic time scale is a power of the length scale, as in the quantum spin- $\frac{1}{2}$ Ising chain, the scaling variable should be $\ln L_\tau / \ln L_\tau^{\max}$ with $\ln L_\tau^{\max} \propto L^\psi$, for some positive constant ψ . As shown in the bottom of Fig. 1C, the data do collapse well for $\psi = 0.37$.

V. CORRELATION FUNCTION

The equal time correlation function,

$$C_{\alpha,i}(r) = [\langle S_{\alpha,i}(\tau) S_{\alpha,i+r}(\tau) \rangle], \quad (8)$$

is calculated at criticality for spins $r = L/2$ apart. As shown in Fig. 2, the distribution of the correlation function, $P(C(L/2))$, is getting broader and broader as L increases. This indicates that the rare events dominate the critical properties of the system.

As a result of the breadth of the distribution, the *average* and *typical* quantities behave differently. The typical correlation function is defined here as the exponential of the average of the logarithm.⁴² In Fig. 3, we show that the average correlation function, $C_{\text{avg}}(L/2)$, falls off as a power law, $C_{\text{avg}}(r) \propto r^{-\eta}$, whereas the typical correlation, $C_{\text{typ}}(L/2)$, has a downward curvature and falls off faster than the average value. Our result is consistent with the existence of a stretched exponential decay, $C_{\text{typ}}(r) \propto e^{-\text{const} \times r^\sigma}$, at the critical point.

VI. LOCAL SUSCEPTIBILITY

We now turn our attention to *off-critical* region and calculate the linear susceptibility, χ_l , in the disordered phase, $J < J_c$. In the imaginary time formalism³⁸

$$\chi_l = \sum_{\tau=1}^{L_\tau} \langle S_{\alpha,i}(0) S_{\alpha,i}(\tau) \rangle. \quad (9)$$

The dynamical exponent, z , can be calculated from the probability distribution of linear local susceptibility. Away from the critical point the distributions for different system sizes are well localized. Close to the critical point, however, the probability distribution of $\ln \chi_l$ gets broader with L as shown in Fig. 4. This broadening of the probability distribution is a strong support for the existence of strongly coupled rare regions in the vicinity of the critical point.

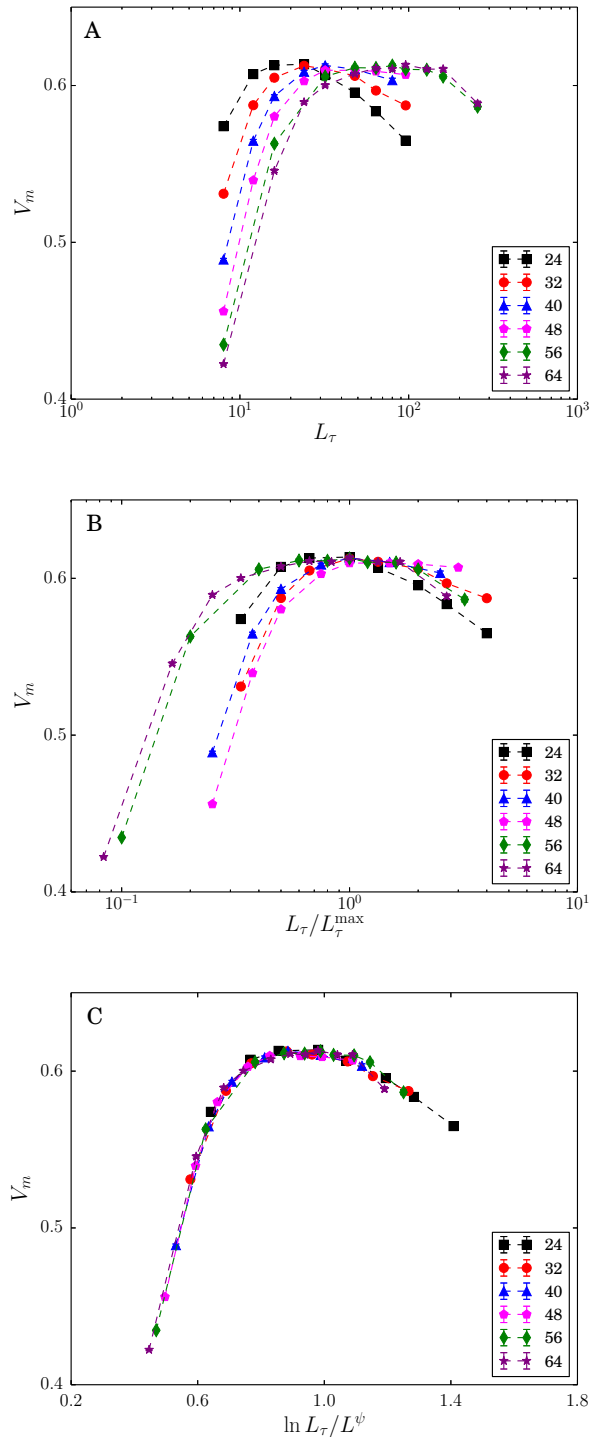


FIG. 1. (Color online) Magnetic Binder cumulant V_m for the parameter set $(K, \Delta_K, \Delta_J) = (0.08, 0.04, 0.2)$ at $J = J_c = 0.245$. Top (A): V_m^{\max} is L independent indicating that the system is at the critical point. Middle (B): the horizontal axis is L_τ/L_τ^{\max} , L_τ^{\max} is the value of the L_τ at the peak. The curves do not scale but get broader for larger system sizes, indicating activated scaling. Bottom (C): V_m versus $\ln L_\tau/L^\psi$ with $\psi = 0.37$. The curves scale well and is consistent with activated scaling. The actual value of ψ is quite uncertain, however, and can range between 0.3 – 0.5.

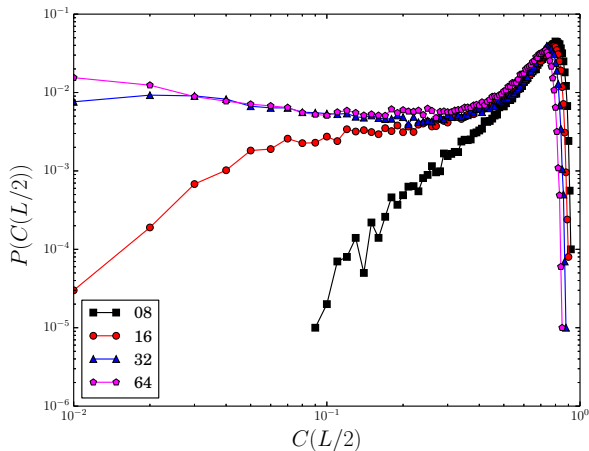


FIG. 2. (Color online) A plot of the distribution of the equal-time correlation of spins $L/2$ apart for the parameter set $(K, \Delta_K, \Delta_J) = (0.08, 0.04, 0.2)$ at $J_c = 0.245$. One sees that the distribution gets broader and broader as L increases. For this plot we used 10^5 realizations of disorder. The values of L_τ are chosen such that $V_m \approx V_m^{\max}$, namely, $L \times L_\tau \in \{8 \times 9, 16 \times 16, 32 \times 37, 64 \times 106\}$.

We examine the behavior of the distribution of local susceptibility following Refs. 15–17, and 43. Given that the probability distribution of logarithm of local susceptibility $P(\ln \chi_l)$ has a power law tail with $P(\ln \chi_l) \propto \chi_l^{-d/z}$, then its integral, $Q(\ln \chi_l) = \int_{\ln \chi_l}^{\infty} P(\ln \chi'_l) d \ln \chi'_l$, behaves similarly to $P(\ln \chi_l)$ with³⁸

$$\ln[Q(\ln \chi_l)] = -\frac{d}{z} \ln \chi_l + \text{const.} \quad (10)$$

It is more accurate to extract the exponent, z , from the cumulative distribution, $Q(\ln(\chi_l))$. In Fig. 4, we show the cumulative distribution of the logarithm of local linear susceptibility.

From the conservation of the probability distribution, we have $\int P(\ln \chi_l) d \ln \chi_l = \int \tilde{P}(\chi_l) d \chi_l$. Therefore $\tilde{P}(\chi) = \chi_l^{-1} P(\ln \chi_l) \propto \chi_l^{-d/z-1}$ and for the average local susceptibility we get

$$\chi_l^{(\text{avg})} \propto \int d \chi_l \chi_l \tilde{P}(\chi_l) = \int d \chi_l \chi_l^{-d/z}. \quad (11)$$

In Fig. 5, we show z as a function of J in the paramagnetic phase. We see that the value of z is larger than 1 for a wide range of J which indicates the divergence of the average local susceptibility in this region; also $z \rightarrow \infty$ as $J \rightarrow J_c \approx 0.245$, compatible with activated dynamical scaling at the criticality.

VII. DISCUSSION

We studied the critical and off-critical properties of the quenched disorder quantum three-color Ashkin-Teller model in $(1+1)$ dimension. Through finite-size scaling analysis of

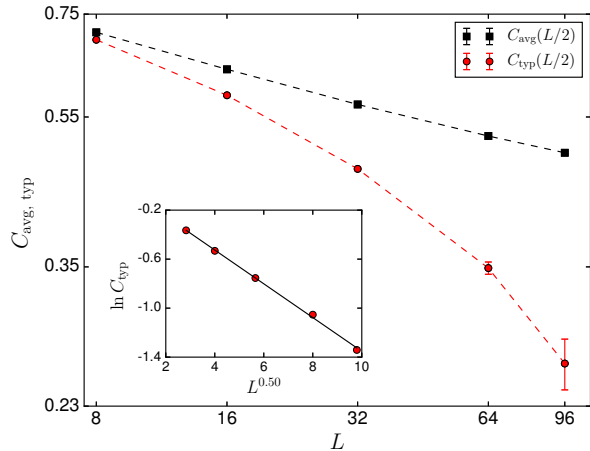


FIG. 3. (Color online) Average and typical correlations between spins $L/2$ apart at criticality, $J_c = 0.245$, for the parameter set $(K, \Delta_K, \Delta_J) = (0.08, 0.04, 0.2)$ (see Fig. 2. Number of disorder realization for the size $L \times L_\tau = 96 \times 224$ is 25×10^3). The average falls off with a power law. The slope of the average correlation function data suggests that $\eta \approx 0.15$. The curvature of the data for the typical correlation function shows that this falls off faster than a power law. The inset shows the linear fit of the logarithm of the typical correlation function against L^σ for the value of $\sigma = 0.50$.

the magnetic Binder cumulant at the quenched disorder induced quantum critical point, we showed that the system exhibits activated scaling. Furthermore, the calculation of the equal time correlation function showed that the rare events dominate the critical properties of the system. This results in a power law behavior of the average quantities, whereas the typical quantities exhibit a stretched exponential decay. We also calculated local susceptibility from which we extracted the dynamical critical exponent and showed the existence of Griffiths-McCoy phase away from the critical point.

Our fitted value of ψ is 0.37, but we cannot rule out a range between 0.3 to 0.5, as already mentioned in the caption of Fig. 1; in Ref. 24 ψ is the same as the strong disorder renormalization group (SDRG), which is 0.5. However, our calculated value of η is 0.15, while in Ref. 24 it is the SDRG value of 0.38. This difference is so large and the linearity (See Fig. 3) is so precise that it seems to be a real effect, not just the sizes being too small in the numerics. Average correlations dominantly come from the rare regions, which are locally in the ordered phase and decay more slowly. Perhaps it is reasonable that there is a much larger probability of being locally in the ordered phase at a first order phase transition. This could be a reason for the smaller value of η . Further work will be necessary to shed light on this issue. The calculation of ν appeared to be computationally prohibitive, especially because of the accuracy demands of our approach; note that one has to calculate correlation function for many different spatial separations and then fit the data.

In summary, the critical behavior of the disorder rounded quantum first-order phase transition of the three color Ashkin-

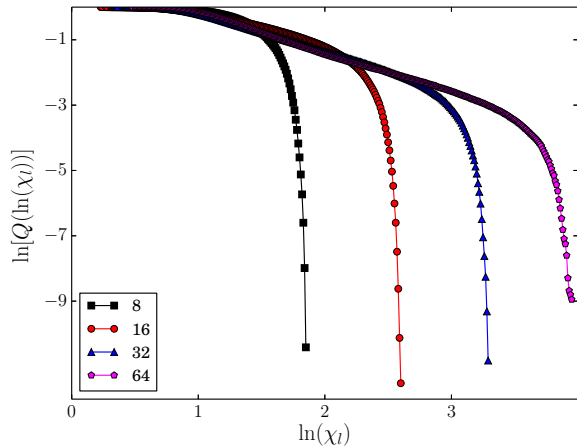


FIG. 4. (Color online) Cumulative probability distribution of $\ln(\chi_l)$ for the parameter set $(K, \Delta_K, \Delta_J) = (0.08, 0.04, 0.2)$ at $J = 0.232$. The distributions get broader as L increases. The slope, $-d/z$, is extracted by performing a linear fit to the linear part of the largest calculated system size, namely for $L = 64$ within the region $1 \leq \ln \chi_l \leq 2.5$.

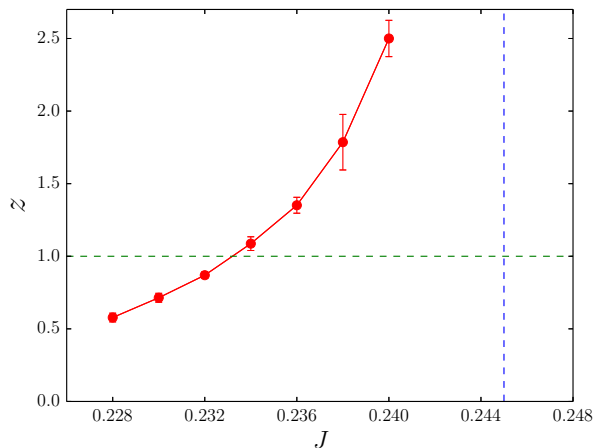


FIG. 5. (Color online) The dynamical exponent z , for different values of J in the paramagnetic phase for the parameter set $(K, \Delta_K, \Delta_J) = (0.08, 0.04, 0.2)$ for our largest lattice size $L = 64$. The blue vertical dashed line is the location of the induced quantum critical point. The horizontal dashed line corresponds to $z = 1$.

Teller model stands out as an example where the effect of disorder in a system is quite complex and considerable care must be exercised in analyzing quantum critical points where material disorder is inevitable.

VIII. ACKNOWLEDGMENT

We are greatly thankful to A.P. Young for important discussions. We also thank the National Science Foundation, Grant No. DMR-1004520 for support.

¹ A. B. Harris, J. Phys. C **7**, 1671 (1974).

² J. T. Chayes, L. Chayes, D. S. Fisher, and T. Spencer, Phys. Rev. Lett. **57**, 2999 (1986).

³ O. Motrunich, S.-C. Mau, D. A. Huse, and D. S. Fisher, Phys. Rev. B **61**, 1160 (2000).

⁴ R. Shankar and G. Murthy, Phys. Rev. B **36**, 536 (1987).

⁵ D. S. Fisher, Phys. Rev. Lett. **69**, 534 (1992).

⁶ T. Senthil and S. N. Majumdar, Phys. Rev. Lett. **76**, 3001 (1996).

⁷ R. A. Hyman and K. Yang, Phys. Rev. Lett. **78**, 1783 (1997).

⁸ S.-k. Ma, C. Dasgupta, and C.-k. Hu, Phys. Rev. Lett. **43**, 1434 (1979).

⁹ C. Dasgupta and S.-k. Ma, Phys. Rev. B **22**, 1305 (1980).

¹⁰ B. M. McCoy and T. T. Wu, Phys. Rev. **176**, 631 (1968).

¹¹ B. M. McCoy and T. T. Wu, Phys. Rev. **188**, 982 (1969).

¹² B. M. McCoy, Phys. Rev. **188**, 1014 (1969).

- ¹³ C. Monthus, O. Golinelli, and T. Jolicœur, Phys. Rev. Lett. **79**, 3254 (1997).
- ¹⁴ D. S. Fisher, Phys. Rev. B **51**, 6411 (1995).
- ¹⁵ H. Rieger and A. P. Young, Phys. Rev. B **54**, 3328 (1996).
- ¹⁶ A. P. Young and H. Rieger, Phys. Rev. B **53**, 8486 (1996).
- ¹⁷ M. Guo, R. N. Bhatt, and D. A. Huse, Phys. Rev. Lett. **72**, 4137 (1994).
- ¹⁸ P. Goswami, D. Schwab, and S. Chakravarty, Phys. Rev. Lett. **100**, 015703 (2008).
- ¹⁹ R. L. Greenblatt, M. Aizenman, and J. L. Lebowitz, Phys. Rev. Lett. **103**, 197201 (2009).
- ²⁰ R. L. Greenblatt, M. Aizenman, and J. L. Lebowitz, Phys. A **389**, 2902 (2010).
- ²¹ F. Hrahsheh, J. A. Hoyos, and T. Vojta, Phys. Rev. B **86**, 214204 (2012).
- ²² A. Bellafard, H. G. Katzgraber, M. Troyer, and S. Chakravarty, Phys. Rev. Lett. **109**, 155701 (2012).
- ²³ A. Bellafard, S. Chakravarty, M. Troyer, and H. G. Katzgraber, Annals of Physics **357**, 66 (2015).
- ²⁴ H. Barghathi, F. Hrahsheh, J. A. Hoyos, R. Narayanan, and T. Vojta, Physica Scripta **T165**, 014040 (2015).
- ²⁵ Y. Imry and M. Wortis, Phys. Rev. B **19**, 3580 (1979).
- ²⁶ K. Hui and A. N. Berker, Phys. Rev. Lett. **62**, 2507 (1989).
- ²⁷ M. Aizenman and J. Wehr, Commun. Math. Phys. **130**, 489 (1990).
- ²⁸ M. Aizenman and J. Wehr, Phys. Rev. Lett. **62**, 2503 (1989).
- ²⁹ G. S. Grest and M. Widom, Phys. Rev. B **24**, 6508 (1981).
- ³⁰ E. Fradkin, Phys. Rev. Lett. **53**, 1967 (1984).
- ³¹ R. Shankar, Phys. Rev. Lett. **55**, 453 (1985).
- ³² H. A. Ceccatto, J. Phys. A **24**, 2829 (1991).
- ³³ R. H. Swendsen and J.-S. Wang, Phys. Rev. Lett. **58**, 86 (1987).
- ³⁴ F. Niedermayer, Phys. Rev. Lett. **61**, 2026 (1988).
- ³⁵ P. Young, *Everything you wanted to know about Data Analysis and Fitting but were afraid to ask*, 1st ed. (Springer, 2015).
- ³⁶ P. Young, (2012), arXiv:1210.3781v2 [physics.data-an].
- ³⁷ C. F. J. Wu, Ann. Stat. **14**, pp. 1261 (1986).
- ³⁸ H. Rieger and A. P. Young, Phys. Rev. Lett. **72**, 4141 (1994).
- ³⁹ K. Binder and D. P. Landau, Phys. Rev. B **30**, 1477 (1984); M. S. S. Challa, D. P. Landau, and K. Binder, *ibid.* **34**, 1841 (1986).
- ⁴⁰ K. Binder, Phys. Rev. Lett. **47**, 693 (1981).
- ⁴¹ K. Binder, Z. Phys. B **43**, 119 (1981).
- ⁴² J. Kisker and A. P. Young, Phys. Rev. B **58**, 14397 (1998).
- ⁴³ F. Iglói, R. Juhász, and H. Rieger, Phys. Rev. B **59**, 11308 (1999).